ORIGINAL ARTICLE

Piperlongumin Improves Survival in the Mouse Model of Sepsis: Effect on Coagulation Factors and Lung Inflammation

Zhendong Fang[1,2,3] , **Xianwei Zhang**[1,2,3] , **Yueyue Huang**[1,2,3] , **Hongmin Zhou**[1,2,3] , **Yilun Lu**[1,2,3] , **Yuanyuan Sun**[1,2,3] , **Fanrong Ye**[1,2,3] , **Songzan Qian**[1,2,3] , **Lingling Pan**[1,2,3] , **Wenjing Chen**[1,2,3] , **Hao Jiang**[1,2,3] and **Jingye Pan**[1,2,3,4,5]

Abstract— Excessive inflammation and coagulation contribute to high morbidity and mortality in sepsis. Many studies have indicated the role of piperlongumine (PL) in anti-inflammation, but its effect on coagulation remains uncertain. Here, we explore whether PL could moderate coagulation indicators and alleviate lung inflammation during sepsis. RAW264.7 cells were induced by lipopolysaccharide (LPS) and treated with PL. Inflammatory and coagulation indicators, cell function and signaling, were evaluated in cells. Cecal ligation and puncture (CLP) mice were treated with PL by gavage. The harvested lungs and plasma were used to assess inflammation and coagulation indicators. As a result, PL increased the survival rate and reduced the concentrations of tissue factor (TF), plasminogen activator inhibitor 1 (PAI-1), thrombin-antithrombin complex (TAT), D-dimer, interleukin (IL)-6, IL-1β, and tumor necrosis factor (TNF)-α in CLP mice, with fibrinogen in reverse. Moreover, the PL alleviated inflammation, fibrin deposition, and lung injury in the lungs of CLP mice. *In vitro*, PL downregulated the expression of TF, PAI-1, IL-6, TNF-α, and IL-1β in RAW264.7 cells induced by LPS. Furthermore, PL inhibited the phosphorylation of the AKT/mTOR signaling pathway's key proteins and suppressed the nuclear translocation of p-STAT3 in LPS-stimulated RAW264.7 cells. In conclusion, this study suggests that PL may modulate coagulation indicators and improve lung inflammation through AKT/mTOR signaling pathway in sepsis.

KEY WORDS: piperlongumine; sepsis; coagulation indicators; lung inflammation; AKT/mTOR.

[1]Department of Intensive Care Unit, The First Affiliated Hospital of Wenzhou Medical University, Wenzhou, China

[2]Key Laboratory of Intelligent Treatment and Life Support for Critical Diseases of Zhejiang Provincial, Wenzhou, China

[3]Wenzhou Key Laboratory of Critical Care and Artificial Intelligence, Wenzhou, China

[4]The Project of Application Technology Collaborative Innovation Center of Wenzhou Institutions of Higher-Learning-Collaborative Innovation Center of Intelligence Medical Education, Wenzhou, China

[5]To whom correspondence should be addressed at Department of Intensive Care Unit, The First Affiliated Hospital of Wenzhou Medical University, Wenzhou, China. Email: wmupanjingye@126.com

INTRODUCTION

Septic patients in intensive care units (ICU) are at risk for life-threatening organ dysfunction due to infection, which affects their survival and prognosis. As pointed out by WHO (2017), there are about 30 million cases of sepsis worldwide each year, and the mortality rate is as high as 20% [1]. Autopsies of patients with sepsis have revealed extensive micro-thrombosis in tissues and organs [2–4]. Activation of the coagulation system is a common phenomenon in sepsis, which leads to disseminated intravascular coagulation (DIC) [5]. According to a previous study, the proportion of sepsis with DIC is 28.9–46.8%, and the mortality rate is as high as 38.4–43% [6]. Therefore, alleviating the disorder of coagulation is the key to decreasing the mortality in sepsis.

Macrophages play a crucial role in sepsis-related lung inflammation, known as acute respiratory distress syndrome (ARDS) [7]. Severe sepsis is characterized by many inflammatory mediators (e.g., interleukin (IL)-6, IL-1β, tumor necrosis factor (TNF)-α) secreted by macrophages [8]. The release of inflammatory factors activates the coagulation system and promotes fibrin production leading to thrombosis [9]. There was a great deal of fluid exuding from the lungs of septic patients, and many microthrombi in the lungs' micro-vessels [4]. In addition, studies have shown that inhibiting the expression of IL-6 or IL-1 can significantly reduce sepsis-induced thrombin production, inhibiting the activation of coagulation, in animal models of sepsis [10, 11]. The thrombin binding to macrophage PAR receptors exacerbates the inflammatory response [12].

Activating the AKT/mTOR signaling pathway in sepsis can lead to inflammatory response and mediate organ dysfunction. Studies have pointed out that the relationship between the activation of AKT/mTOR and the expression of tissue factors (TF) has been confirmed [15, 16]. Additionally, STAT3, a nuclear transcription factor, is regulated by the AKT/mTOR signaling pathway [17]. It is also possible to suppress the expression of tissue factor (TF) by inhibiting transcription factor STAT3 [18]. TF initiates the exogenous coagulation pathway and the core element of coagulation activation in sepsis [19]. Typically, TF is expressed at low levels *in vivo*. During sepsis, sustained activation of TF triggers the extrinsic coagulation pathway that increases fibrin production [9]. The activation of coagulation promotes fibrinolysis, which in turn causes fibrin degradation and elevates D-dimer (D-D) levels. This process will result in higher levels of plasminogen activator inhibitor 1 (PAI-1), and the excessive secretion of PAI-1 will impair fibrinolysis [20]. Coagulation disorders are a result of this series of processes.

Piperlongumine (PL) is a natural alkaloid derived from the root of the Piperaceae plant *Piper longum*. Previous studies have demonstrated its analgesic, antitumor, reducing macrophage adhesion, and potentially inhibiting platelet aggregation [21–24]. Additionally, it has been suggested that PL can inhibit the activation of the AKT/mTOR signaling pathway to alleviate inflammation [25]. In sepsis, inflammation and coagulation promote each other. However, the effect of PL on coagulation indicators remains uncertain. Here, we explore the potential relation between PL, lung inflammation, and coagulation indicators during sepsis.

MATERIALS AND METHODS

Cell Culture

DMEM (Gibco, Germany) with 10% fetal bovine serum (FBS, Sigma, USA) was used to culture RAW264.7 (ATCC, USA) cells at a 37 °C and 5% CO_2 incubator. RAW264.7 cells were seeded on six-well plates with 1×10^6 cells/well and incubated at 37 °C with 5% CO_2 until 60–70% confluence was reached. The control group was treated with dimethyl sulfoxide (DMSO, 0.25 μL/mL), used for dilution of PL. The PL group was treated with 2.5 μM piperlongumine (PL, 20,069–09-4, MCE, USA). The LPS group was treated with 1 μg/mL lipopolysaccharide (LPS, Escherichia coli O127:B8, Sigma, USA) for 6 h [26]. The LPS + PL group was treated with 2.5 μM PL for 2 h, followed by 1 μg/mL LPS for 6 h.

Preparation of PL

For *in vivo* experiments, PL was dissolved in 80% corn oil + 20% DMSO (10 mg/mL). For *in vitro* experiments, dissolve PL in DMSO to prepare a stock solution at a concentration of 5 mM. The above solution was stored at −80 °C.

Experimental Animals

Shanghai SLAC Laboratory Animal Limited Liability Company (Shanghai, China) provided male C57BL/6 mice (aged 8–10 weeks). In a 12-h dark/light cycle pathogen-free facility, mice were raised at $55 \pm 10\%$ humidity and 23 ± 3 °C

temperature. Food and water were always accessible. All animal care and tests were carried out with Wenzhou Medical University's Animal Care and Use Committee.

Cecal Ligation and Puncture (CLP)

According to the random number table method, mice were divided into three groups: sham group, CLP group, and CLP + PL group. There were more than six samples in each group after the processing time, and each sample was repeated three times. Before the surgical procedure, the mice were anesthetized with 1% sodium pentobarbital (100 μL/10 g; Solarbio, China) through intraperitoneal injection. Then, we incised the abdominal cavity to find the cecum, ligated it 1 cm from the end, punched twice with a 21-gauge needle, and squeezed a small amount of feces into the abdominal cavity. Finally, the cecum was put back, and the abdominal wall was sutured [27]. The mice in the sham group only had their abdominal wall open and administrated with 200 μL dilution (80% corn oil + 20% DMSO), but they performed no other surgical procedures. After the surgical procedure, all mice were injected subcutaneously with 1 mL of saline for fluid resuscitation. A total of 200 μL of PL (10 mg/kg) was administrated by gavage to the mice 2 h before CLP in the CLP + PL group mice. Twenty-four hours later, lung tissues and blood samples were collected. The right lung was used for homogenate (western blot), and the left was for histology (HE and IHC). Blood was harvested through eyeball enucleation and transferred into a sodium citrate (3.2%, 50 μL) anticoagulation tube. Subsequently, plasma was isolated from the blood by centrifugation at $1000 \times g$ for 15 min at 4 °C. In addition, survival analysis was also done to assess the effect of PL on mortality in the sepsis model. Mice in each treatment group ($n = 12$/group) were assessed every 12 h for the following 4 days.

Collection of Bronchoalveolar Lavage Fluid (BALF) in Mice

Twenty-four hours after surgical procedure, the lungs were slowly injected with 1 mL of phosphate-buffered saline (PBS), the thorax was gently squeezed for about 3 s, and the solution was then withdrawn. The above operation was repeated 3 times. The supernatant was discarded after centrifuging the recovered solution at $1500 \times g$ for 10 min at 4 °C. The red blood cells were removed using the Red Blood Cell Lysis Buffer (Beyotime, C3702). The total number of cells in the BALF was counted with a cell counting plate.

ELISA

ELISA kits were performed to determine the concentrations of IL-6, IL-1β, TNF-α, and PAI-1 in logarithmic growth phase cell supernatants, and IL-6, IL-1β, TNF-α, PAI-1, TF, D-dimer, TAT, and fibrinogen in mouse plasma. The experimental process was carried out according to the instructions corresponding to the indicators. The reagent kits are as follows: IL-6 (70-EK206, Multi Science, China), IL-1β (70-EK201B, Multi Science, China), TNF-α (70-EK282, Multi Science, China), TF (DY3178-05, R&D systems, USA), PAI-1 (DY3828-05 R&D systems, USA), D-dimer (CSB-E13584m, Cusabio, China), fibrinogen (CSB-E08202m, Cusabio, China), and TAT (CSB-E08433m, Cusabio, China).

Hematoxylin and Eosin (H&E) Staining of Lung Tissue

The obtained lung tissue samples were dehydrated, embedded, and sectioned after being fixed in 4% paraformaldehyde. Finally, the lung tissue was stained with HE by the instructions of the HE staining kit (Solarbio, China). The severity of lung damage can also be determined by assessing the presence or absence of interstitial inflammation, neutrophil infiltration, congestion, and edema. The following scores were assigned to lung injury: 0 (no injury); 1 (injury in 25% of the field); 2 (injury in 50% of the field); 3 (injury in 75% of the field); and 4 (injury throughout the field). Ten microscopic fields from each slide were evaluated, and the scores were averaged.

Immunofluorescence

After deparaffinization and hydration of the lung slices with xylene and absolute ethanol, antigen retrieval was performed with 0.01 M sodium citrate buffer (pH 6.0). Then, they have blocked with 5% BSA (Bovine albumin) solution for half an hour and incubated with F4/80 (Santa Cruz, sc-377009) antibody at 4 °C overnight. The next day, after rewarming, we incubated the sections with Alexa Fluor–labeled secondary antibody for 1 h and finally mounted the sections with an anti-fluorescence quencher containing DAPI.

RAW264.7 cells were cultured on a cell slide in six-well plates with 1×10^4 cells/well. PL was added for 2 h, and 1 mg/mL LPS was added for 6 h, and then the treatment was over. Four percent paraformaldehyde was used for fixation, and PBS containing 0.5% Triton-100 was used for

permeabilization and sealing with 5% BSA solution. After incubation overnight with p-STAT3 (9145S, CST, USA) antibody in a refrigerator at 4 °C, the slides were mounted in the same way the next day. Finally, we used a laser confocal microscope (Nikon, Japan) to observe the fluorescence signal in tissues and cells. Mean fluorescence intensity (MFI) was used to estimate the statistical significance.

Cell Counting Kit-8 (CCK-8) Assay

As a measure of cell viability, RAW264.7 cells were seeded on 96-well plates with 100 μL medium, attached overnight, and then analyzed by the CCK8 assay (MCE, USA). PL was added to cells at 0, 0.625, 1.25, 2.5, 5, 10, and 20 μM concentrations, and they were incubated at 37 °C with 5% CO_2. The group in 0 concentration was treated with DMSO. After 24 h, 10 μL of CCK8 solution was added to each well (6 wells/group) and incubated in a 37 °C incubator for 2 h. Finally, using a microplate reader set to 450 nm, each well's optical density (OD value) was determined. Each group had six wells, and every experiment was performed in triplicates independently.

Western Blotting

Lyse of lung tissue and RAW264.7 cells was carried out using RIPA buffer (Beyotime, China) with 10% protein phosphatase inhibitor (Roche, Switzerland). BCA kit (Thermo Fisher, USA) measured protein concentration. On a 10–12.5% SDS-PAGE gel, 20 μg protein samples were separated and transferred to the PVDF membrane (EDM Millipore, Billerica, MA). After that, the membranes were blocked with 5% non-fat milk in TBST buffer (1*TBS, 0.1% Tween 20) for 2 h at room temperature. Incubation of the membranes with the primary antibody at 4 °C overnight followed. Here are the primary antibodies: p-AKT (Ser473) (1:2000, 4060S), AKT (1:1000, 4691S), p-STAT3 (Try705) (1:2000, 9145S), STAT3 (1:1000, 9139S), p-NF-κB p65 (Ser536) (1:1000, 3033 T), NF-κB p65 (1:1000, 8242 T), p-IκB-α (Ser32) (1:1000, 2859 T), IκB-α (1:1000, 4814 T), p-mTOR (Ser2448) (1:1000, 5536S), and mTOR (1:1000, 2983 T) from Cell Signaling Technology, USA. TF (1:1000, DF6400), IL-6 (1:1000, DF6087), TNF-α (1:500, AF7014), IL-1β (1:1000, AF5103), GAPDH (1:10,000, AF7021), tubulin (1:3000, AF7011), and histone (1:2000, BF9211) are from Affinity, USA. GAPDH, tubulin, and histone were internal reference proteins in this study. The next day,

membranes were incubated with (HRP)-conjugated goat anti-rabbit IgG antibody (1:1000, A0216, Beyotime, China) or anti-mouse IgG antibody (1:1000, A0208, Beyotime, China) for 1 h at room temperature. Then, the membranes were detected with an ECL chemiluminescence reagent (Thermo Fisher, USA). Finally, ImageJ (NIH, USA) was used to quantify the specific bands.

RNA Isolation and Quantitative Real-Time PCR

Total RNA was extracted from RAW264.7 cells using RNAsimple total RNA kit (Tiangen, China). 5×All-In-One RT MasterMix (ABM, Canada) converts 1000 ng RNA to cDNA, with a final volume of 20 μL, by the instructions. Next, SYBR Green (Torovid, China) and PCR detection systems (7500fast; USA) were used to analyze the relative expression of target gene mRNA in the samples (using GAPDH as an internal reference). The thermal cycling parameters were as follows: initial denaturation at 95 °C for 60 s, denature at 95 °C for 15 s, anneal at 60 °C for 30 s, and extension at 72 °C for 45 s, and then denature-anneal-extension cycling for 40 times. The $2^{-\Delta\Delta Ct}$ method was used to analyze the results statistically. All primer sequences are shown in Table 1.

Statistical Analysis

Every experiment was performed in triplicates independently. Values are shown as mean ± SD. *In vivo*, each group was composed of six mice randomly selected.

Table 1 Real-Time (RT)-PCR Primers

Primer		Primer sequence
GAPDH	Forward	GGAGCGAGATCCCTCCAAAAT
	Reverse	GGCTGTTGTCATACTTCTCATGG
IL-6	Forward	CAATAACCACCCCTGACC
	Reverse	GCGCAGAATGAGATGAGTT
IL-1β	Forward	GCTGCTTCCAAACCTTTGAC
	Reverse	CTTCTCCACAGCCACAATGA
TNF-α	Forward	GGAAAGGACACCATGAGC
	Reverse	CCACGATCAGGAAGGAGA
TF	Forward	CCAAACCCGTCAATCAAGTC
	Reverse	TCTGCTTCACATCCTTCACAAT
PAI-1	Forward	CTTCCACCCGTCTCTCTG
	Reverse	CTACCAGGCACACAAAAGC

Data were statistically analyzed using GraphPad Prism 8.4.2 (GraphPad Software, USA). The study analyzed differences between three or more groups using one-way ANOVA followed by Tukey's as a post hoc multiple comparison test. Each set of data was obtained by conducting at least three independent experiments. P values in all figures were indicated as $^*P < 0.05$ and $^{**}P < 0.01$ versus control group; $^#P < 0.05$ and $^{##}P < 0.01$ versus LPS group.

RESULTS

PL Improves Survival Rate and Moderates Coagulation and Inflammation Indicators in CLP Mice

To verify the protective effect of PL in CLP mice, survival analysis was performed. A 96-h survival rate of 16.7% (7/12) was recorded for the CLP group whereas a survival rate of 41.6% (5/12) was recorded for the CLP + PL group. PL treatment significantly decreased mortality in CLP mice (Fig. 1A).

To explore whether PL reduces coagulation and inflammation indicators in CLP mice, we used ELISA kits to determine the concentration of plasma coagulation and inflammation indicators. There were significantly higher levels of TF, PAI-1, TAT, D-dimer, IL-6, IL-1β, and TNF-α in the plasma of the CLP group than that of the sham group (Fig. 1B–H). As expected, PL markedly decreased the concentration of the above markers in CLP mice (Fig. 1B–H). In addition, fibrinogen concentration was effectively decreased in the CLP mice compared to the sham group (Fig. 1I). The pharmacological intervention with PL reversed the trends of fibrinogen in CLP mice plasma.

PL Alleviates Inflammation and Fibrin Deposition in the Lungs of CLP Mice

Histopathological examination of lung tissues was conducted to study the effect of PL on lung injury. Compared with the sham group, the lung sections in the untreated CLP mice showed that the pulmonary interstitial edema was severe, the septal wall thickened, the inflammatory cell infiltration increased, and the lung injury score increased (Fig. 2A, B). By administering PL, these manifestations were alleviated (Fig. 2A, B). In addition, pretreatment with the PL markedly reduced fibrin deposition in the lungs during sepsis, as revealed by

immunohistochemical detection (Fig. 2C). Lung homogenates were tested for inflammatory cytokines, including TNF-α, IL-6, and IL-1β (Fig. 2D). PL treatment showed a significant reduction of TNF-α, IL-6, and IL-1β in the lungs compared to the CLP group. Macrophages play a vital role in sepsis pathogenesis. The F4/80 labeling of macrophages in mouse lung tissue showed that PL effectively reduced increased macrophage infiltration in septic lung tissue (Fig. 3A, B). The total cells were measured in the BALF. The count of total cells in the BALF was higher in the CLP group than the sham group, while it decreased with PL administration (Fig. 3C). In the lungs of CLP mice, phosphorylation of AKT, mTOR, and STAT3 was significantly increased, and PL treatment diminished its effects (Fig. 3D-G).

Screening the Appropriate Concentration of PL

CCK-8 assay was used to test the cell viability in different concentrations of PL. According to Fig. 4A, PL did not affect the viability of RAW264.7 cells when the concentration ranged from 0 to 2.5 μM (Fig. 4A). When the concentration of PL was greater or equal to 5 μM, the cell viability of RAW264.7 decreased. Through IC50 analysis, we found that the cell survival rate decreased to 50%, while the concentration of PL reached 4.899 μM (Fig. 4B). In the group treated with LPS for 6 h, IL-1β and TNF-α mRNA levels were significantly elevated (Fig. 4C, D). The mRNA levels of IL-1β and TNF-α in the LPS + PL group were significantly reduced dose-dependent compared to the LPS group. Therefore, we chose 2.5 μM as the subsequent application concentration of PL.

PL Suppresses the Inflammation in RAW264.7 Cells

To confirm the inhibitory effect of PL on inflammation, RAW264.7 cells were treated with PL 2 h before LPS stimulation. As a result, PL pretreatment significantly reduced LPS-induced mRNA levels of TNF-α, IL-6, and IL-1β in RAW264.7 cells (Fig. 5A–C). In the LPS group, higher concentrations of TNF-α, IL-6, and IL-1β were detected in the supernatant than in the control and PL groups (Fig. 5D–F). However, the concentrations of these biomarkers in the supernatant were effectively decreased in the LPS + PL group compared to the LPS group (Fig. 5D–F). Furthermore, dysregulated activation of the NF-κB pathway plays a role in the pathogenesis of
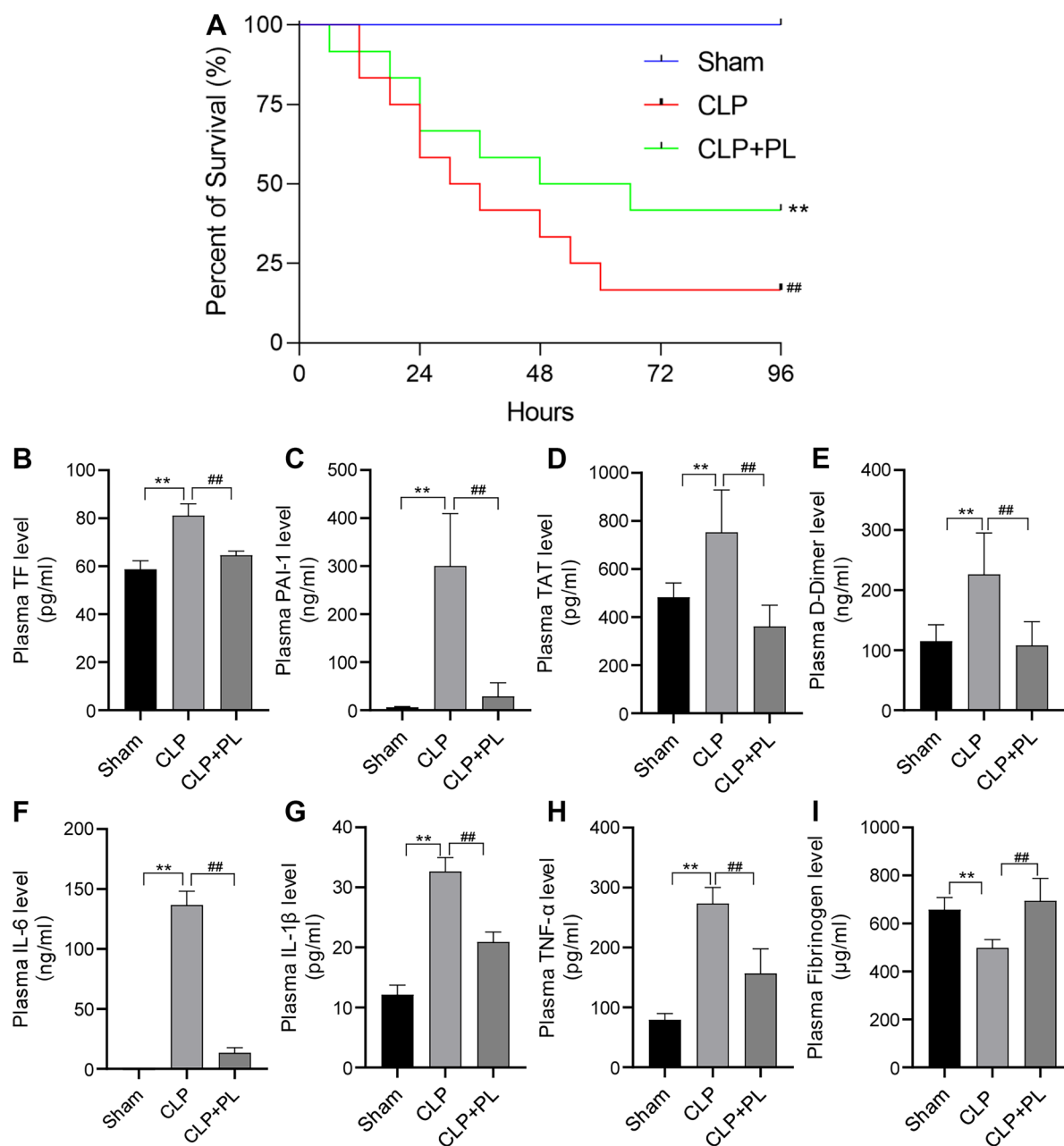
Fig. 1 PL improves survival rate, coagulation, and inflammation indicators in CLP mice. **A** It is a survival analysis for the experimental mice ($n = 12$ mice per group; Kaplan–Meier survival analysis). **B–I** Using ELISA kits in mice plasma, TF, PAI-1, TAT, D-dimer, IL-6, IL-1β, TNF-α, and fibrinogen concentrations were determined ($n = 6$/group). Values are shown as mean ± SD. $^{**}P < 0.01$ versus sham group; $^{##}P < 0.01$ versus CLP group.
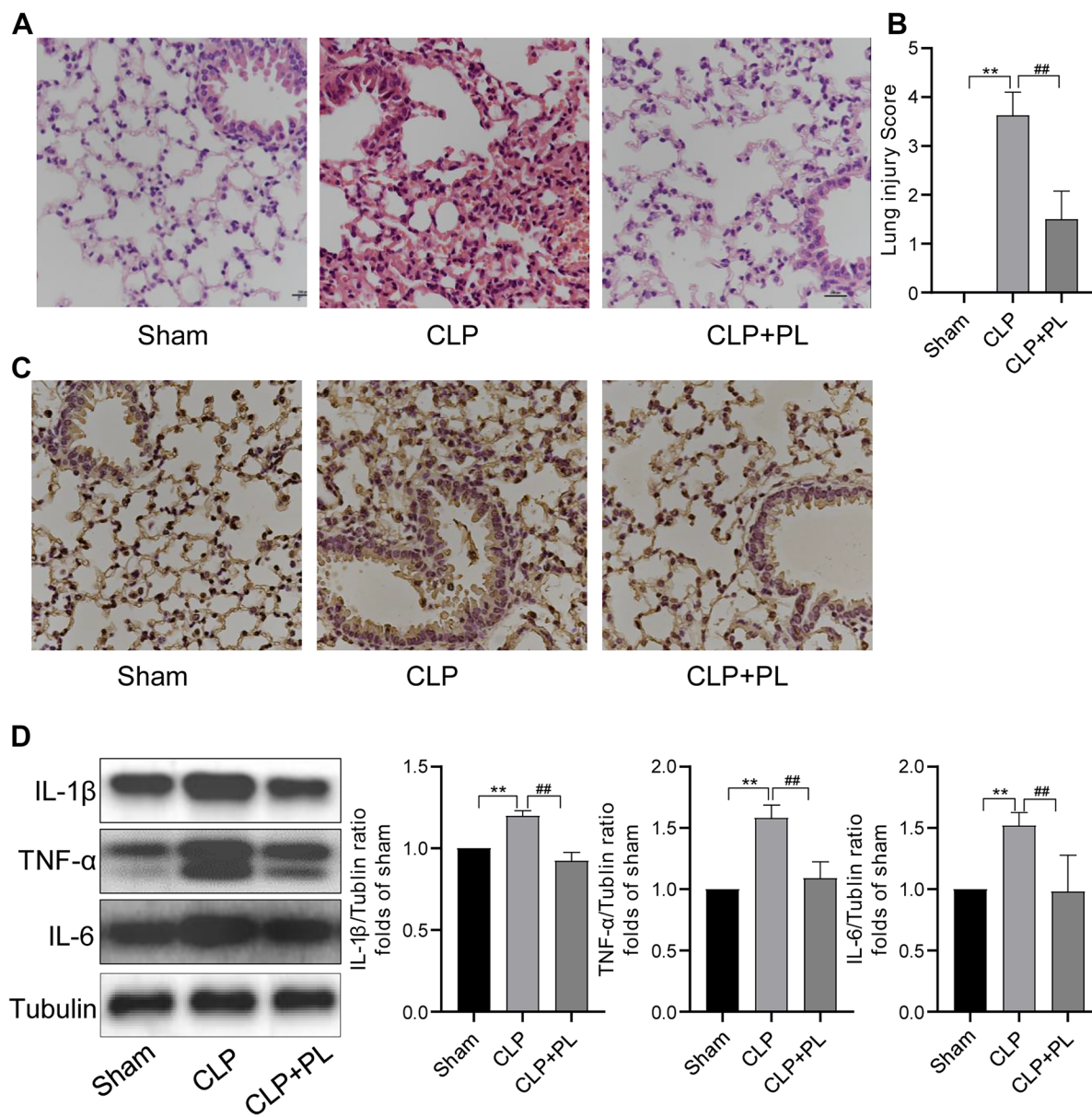
Fig. 2 PL alleviates inflammation and fibrin deposition in the lungs of CLP mice. **A** HE-stained images of lungs in each group were observed under an optical microscope (scale bar: 10 μm). **B** Lung injury score was evaluated according to the degree and scope of lung injury, including the degree of interstitial edema, septal wall thickness, and inflammatory cell infiltration. **C** Representative images of immunohistochemical staining of fibrin were obtained in the lungs from three groups of mice (400×). **D** The western blot results showed IL-1β, TNF-α, and IL-6 protein levels in lung tissues, and the relative expression levels of IL-1β, TNF-α, and IL-6 normalized to tubulin. Values are shown as mean ± SD. $^{**}P < 0.01$ versus sham group; $^{##}P < 0.01$ versus CLP group.
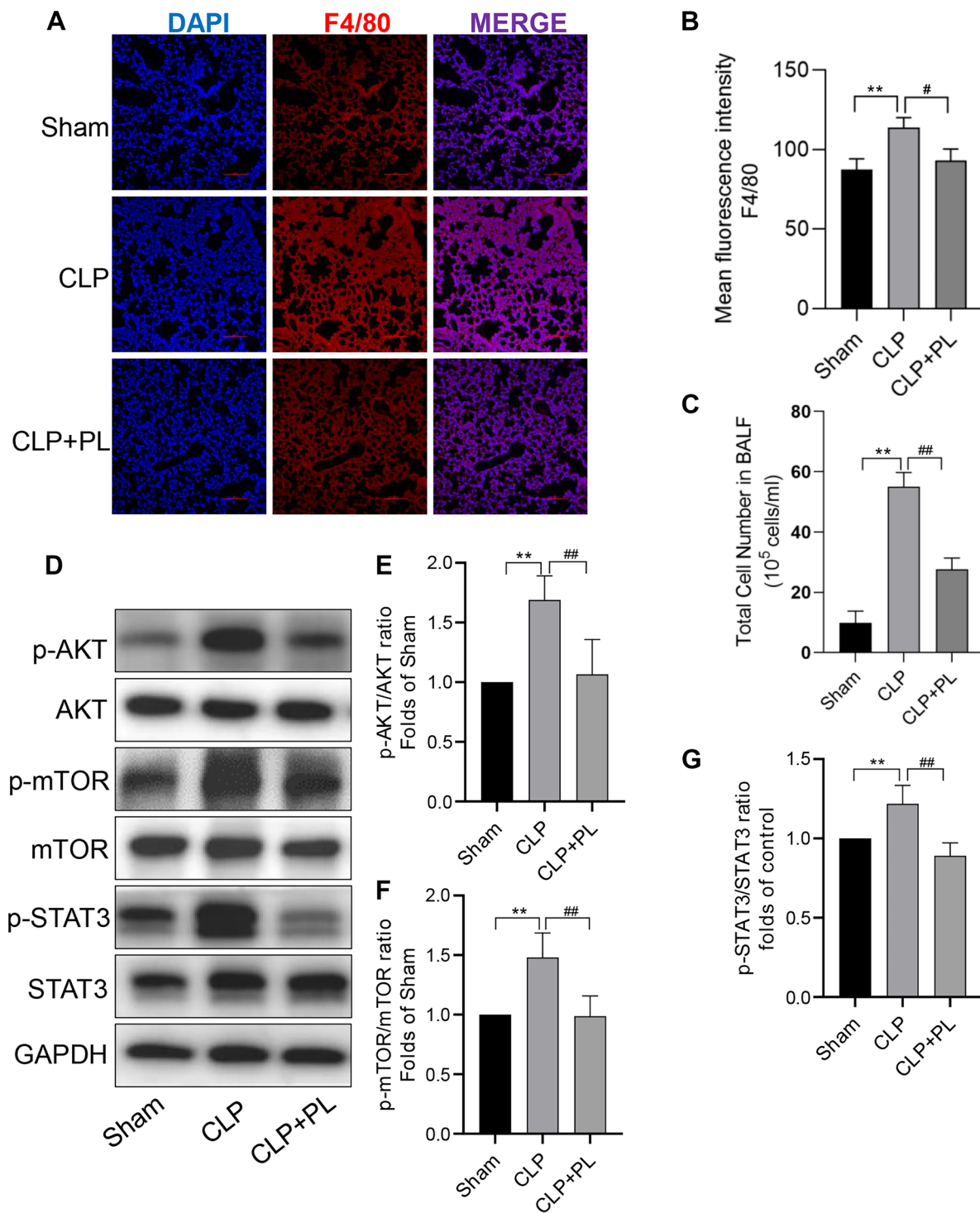
◀ **Fig. 3** PL inhibited macrophage infiltration and AKT/mTOR/STAT3 activation in the lungs of CLP mice. **A**, **B** F4/80 (red) fluorescence images of lung tissue were taken under a confocal laser microscope (scale bar: 100 μm). **C** Total cell numbers in BALF were calculated with cell counting plate. **D**–**G** The western blot results showed phosphorylation levels of AKT, mTOR, and STAT3 in lung tissues. Values are shown as mean $\pm$ SD. $^{**}P < 0.01$ versus sham group; $^{\#}P < 0.05$, $^{\#\#}P < 0.01$ versus CLP group.

inflammation [28]. While treating RAW264.7 cells with 1 μg/mL LPS increased the phosphorylation of NF-κB p65 and IκBα, pretreatment with PL (2.5 μM) considerably inhibited this phosphorylation in LPS-induced macrophages. These results suggest that PL suppresses the inflammation through the NF-κB signaling pathway *in vitro* model.

PL Reduces the Surge in TF and PAI-1 in Macrophages Stimulated by LPS Through AKT/mTOR/STAT3 Signaling Pathway

TF and PAI-1 are essential indicators of coagulation. Hence, the effect of PL on TF and PAI-1 was investigated. Elevations in the mRNA levels of PAI-1and TF stimulated by LPS were reversed upon PL treatment (Fig. 6A–B). Compared with the control and PL group, PAI-1 in cell supernatant was markedly increased after LPS stimulation (Fig. 6C). Supernatant PAI-1 levels of the LPS + PL group were decreased compared to the LPS group (Fig. 6C). To further determine whether PL downregulates TF protein levels, TF in RAW264.7 cells was detected by western blot. While TF level was significantly enhanced in the LPS group compared to the control and PL group, the expression of TF was effectively decreased by PL treatment (Fig. 6D, E). Besides, the relative pathway in RAW264.7 cells was checked, and PL reduced the phosphorylation of AKT, mTOR, and STAT3 triggered by LPS (Fig. 6G–I). Therefore, these results demonstrated that PL attenuated the TF and PAI-1 through AKT/mTOR/STAT3 signaling pathway in RAW264.7 cells.

PL Inhibits the Translocation of p-STAT3 into the Nucleus after LPS Stimulation in RAW264.7 Cells

We wonder whether PL exerts the anti-coagulation by inhibiting p-STAT3 nuclear translocation in LPS-induced RAW264.7 cells. Extracts of nuclear proteins were used to detect p-STAT3 distribution in the nucleus. The nuclear p-STAT3 significantly enhanced in LPS-induced RAW264.7 cells, while PL markedly reduced LPS-treated p-STAT3 nuclear translocation (Fig. 7A). These findings were further supported by immunofluorescence staining. As a result, the mean fluorescence intensity of p-STAT3 in RAW264.7 was increased by LPS stimulation but weakened in the presence of PL (Fig. 7B).

DISCUSSION

Inflammatory storm and coagulation disorders caused by sepsis or septic shock are the main causes of ICU morbidity and mortality. Although several strategies have been used to treat patients with sepsis, no specific therapeutic agent is available to manage sepsis. Therefore, developing drugs that can alleviate inflammation and coagulation disorders is essential for sepsis treatment [29]. This study shows that PL effectively increased the survival rate of CLP mice and improved coagulation indicators and lung inflammation caused by sepsis. Moreover, the potential mechanisms were elucidated through the *vivo* and *vitro* experiments.

Macrophages are the most important cells in the body's nonspecific immune system, found in various tissues and organs, including the lung, liver, and brain [30]. Macrophages also involve pathophysiological responses induced by sepsis, such as inflammatory storms, coagulation disorders, and immune imbalance [31–33]. Activation of the inflammation precedes the activation of coagulation. Animal model studies have shown that blocking IL-6 or IL-1 expression significantly inhibits sepsis-induced coagulation and thrombin production [10, 11]. Injection of low doses of LPS in healthy volunteers resulted in a rapid increase in the expression of TF mRNA derived from mononuclear macrophages with increasing in thrombin, TAT, and other coagulation-related markers in plasma [34]. *In vitro*, data showed that PL could reduce the expression of inflammatory mediators and TF in LPS-treated RAW264.7 cells. *In vivo*, treatment with PL significantly reduced the concentrations of inflammatory mediators and TF in CLP mice.

A systemic inflammatory response during sepsis can cause oxidative stress, damaging tissues and organs like the lungs and kidneys [35–39]. ROS-stimulated NLRP can activate the caspase-1/calpain pathway, which can specifically cut off the connection between TF and cell membrane and promote the increase in TF levels
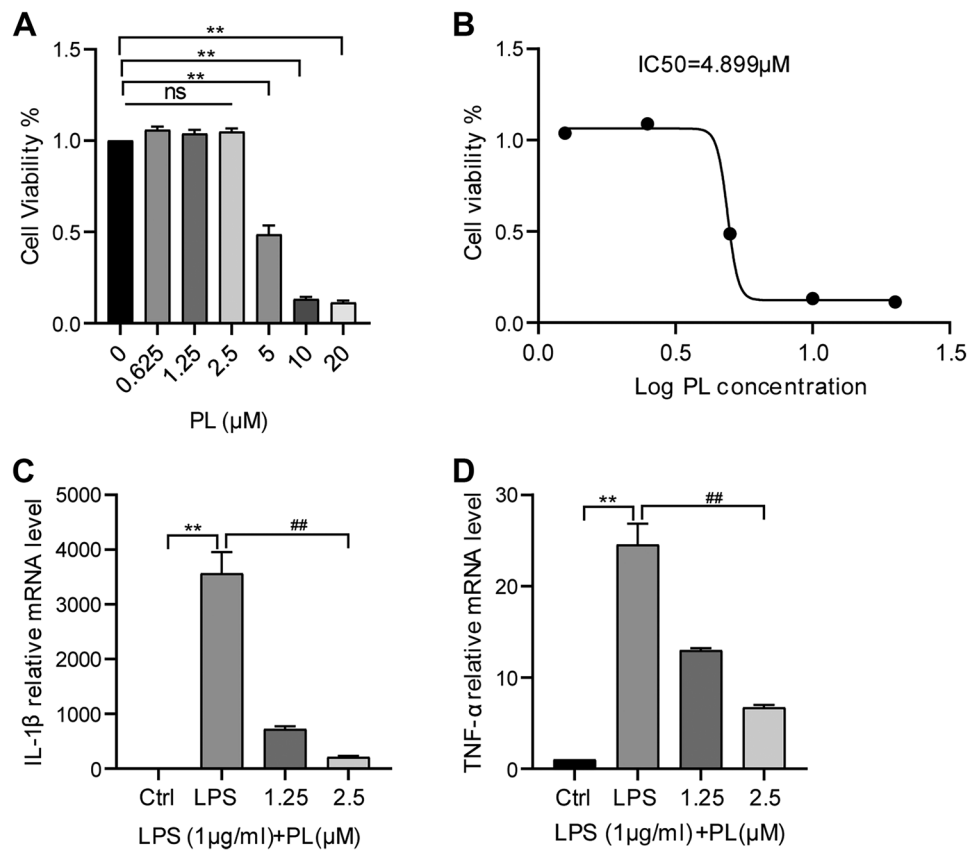
Fig. 4 Screening the appropriate concentration of PL. **A** The CCK-8 assay detected the viability of RAW264.7 cells at different concentrations of PL. **B** Half maximum inhibitory concentration of PL that inhibits RAW264.7 cells. **C, D** PL (1.25 or 2.5 μM) was added 2 h before LPS (1 μg/mL, 6 h) treatment, and the qRT-PCR was used to assess the relative mRNA levels of IL-1β and TNF-α. Every experiment was repeated three times. Values are indicated as mean ± SD. $^{**}P < 0.01$ versus control group; $^{##}P < 0.01$ versus LPS group; NS, not significant versus control group.

in plasma [40]. In addition, Lu Ben *et al*. point out that activation of Caspase-11/GSDMD causes phosphatidylserine (PS) on the inner surface of the cell membrane to invert, and the exposed PS can activate TF [41]. As long as TF is continuously expressed and activated, it will activate coagulation factor VII and combine with it to form a TF-FVIIa complex, initiating the coagulation cascade [42]. These processes will lead to abnormal changes in coagulation indicators, such as TAT, D-dimer, fibrin, and PAI-1, leading to coagulation disorders [3]. This study verified that PL treatment significantly reduced plasma concentrations of TF, PAI-1, TAT, and D-dimer and significantly increased plasma fibrinogen concentrations in CLP mice. Thus, we hypothesize that PL may improve changes in coagulation indicators in plasma of CLP mice by inhibiting TF expression.

The lungs are the most vulnerable organ in sepsis, leading to acute lung inflammation [43–45]. In autopsies of patients with COVID-19 sepsis, it was found that there were transparent membranes in the alveoli and a large number of microthrombi in the pulmonary microvessels [4]. *In vivo*, we observed interstitial lung edema with thickening and disruption of the alveoli structure through lung tissue HE staining. Also, lung tissue damage scores were significantly higher than the sham group. PL intervention alleviated the above pathological changes and reduced lung tissue damage scores. It reduced the infiltration of inflammatory factors, such as IL-6, TNF-α, and IL-1β, in the CLP mice lung tissues. Moreover, total cells were counted in BALF, and F4/80 staining was performed to label macrophages in lung tissue. The results showed that PL could reduce total
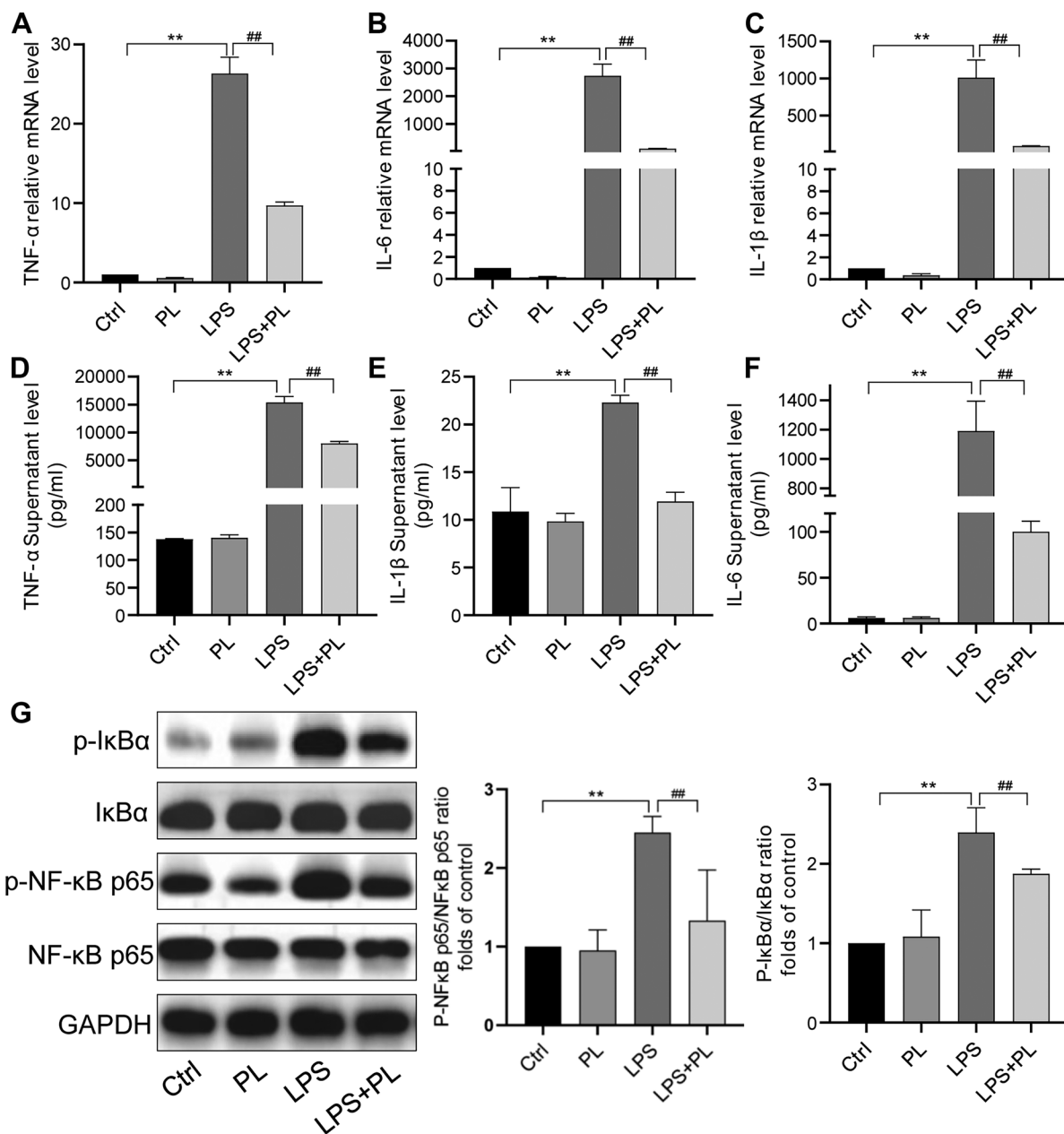
Fig. 5 PL suppresses the inflammation in RAW264.7 cells induced by LPS. **A–C** PL (2.5 μM) was added 2 h before LPS (1 μg/mL, 6 h) treatment, and each group's mRNA expression levels of TNF-α, IL-6, and IL-1β were analyzed by qRT-PCR. **D–F** ELISA analysis of TNF-α, IL-6, and IL-1β concentrations in RAW264.7 supernatant. **G** The western blot results show phosphorylation levels of NF-κB p65 and IκBα in LPS-stimulated RAW264.7 cells. Every indicator was detected three times. Values are indicated as mean ± SD. $^{**}P < 0.01$ versus control group; $^{#}P < 0.05$, $^{##}P < 0.01$ versus LPS group.

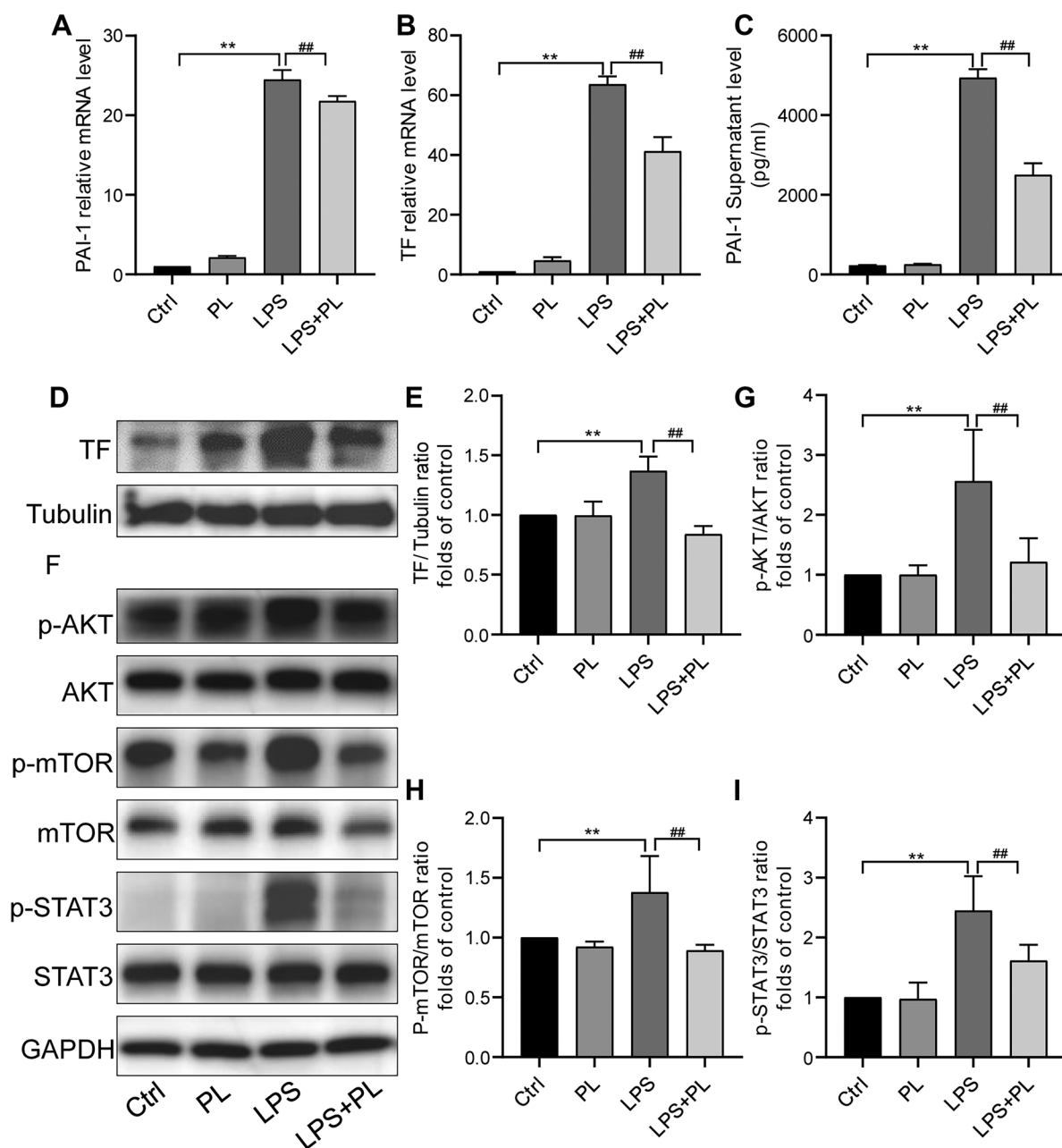**Fig. 6** PL reduces the surge in TF and PAI-1 in macrophages stimulated by LPS. **A**, **B** Each group was tested using qRT-PCR to detect TF and PAI-1 mRNA levels. **C** ELISA determined concentrations of PAI-1 in the supernatant of the RAW264.7 cell. **D**, **E** Western blot analysis showed protein levels of TF in RAW264.7 cells. **F–I** AKT, mTOR, and STAT3 phosphorylation was detected by western blot in RAW264.7 cells. Every experiment was repeated three times. Values are indicated as mean $\pm$ SD. $**P < 0.01$ versus control group; $\#\#P < 0.01$ versus LPS group.
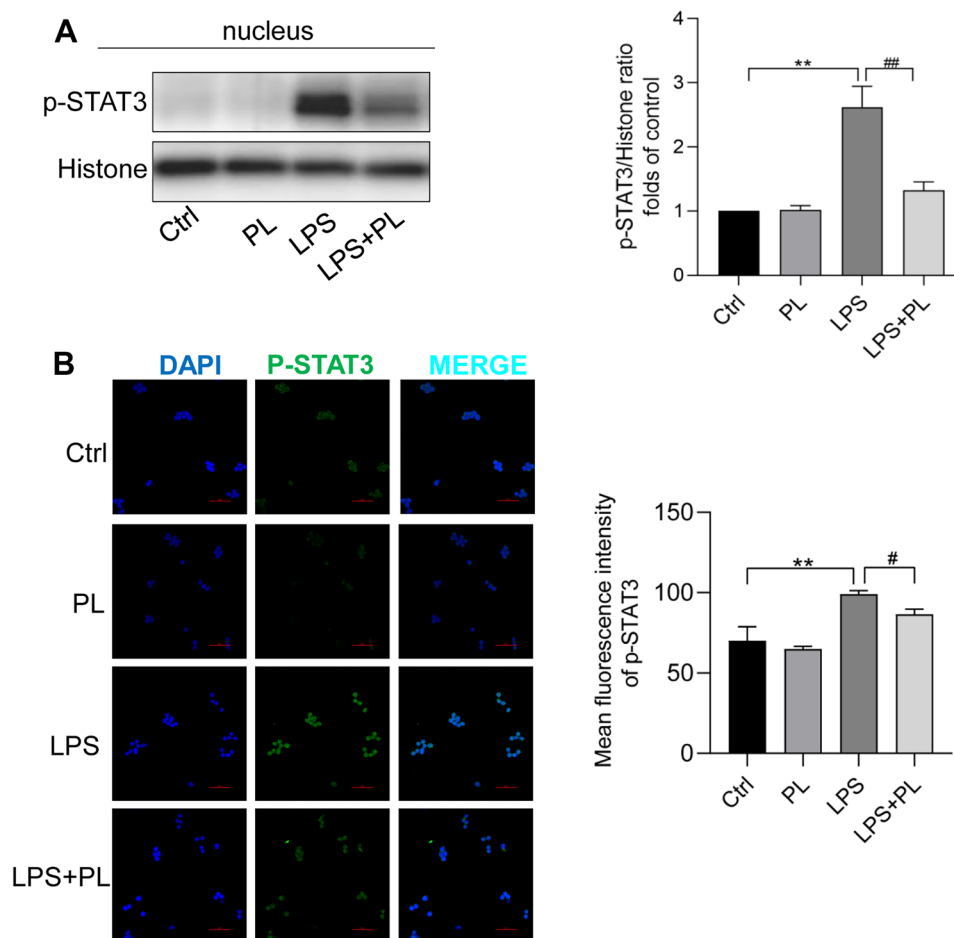
Fig. 7 PL inhibits the translocation of p-STAT3 into the nucleus after LPS stimulation in RAW264.7 cells. **A** The western blot results showed p-STAT3 protein levels in the nucleus of RAW264.7 cells and the relative expression levels of p-STAT3 normalized to histone. **B** The staining of p-STAT3 (green) and nuclei (blue) in RAW264.7 cells was observed by laser confocal microscopy (scale: 5 μm). Values are shown as mean ± SD. $^{**}P < 0.01$ versus control group; $^{#}P < 0.05$, $^{##}P < 0.01$ versus LPS group.

cells and macrophage infiltration in CLP mice lungs. Hence, these results suggested that PL effectively alleviates lung inflammation in CLP mice. In addition, inflammatory responses can activate the coagulation system and promote fibrin formation [9]. Our data indicated that PL markedly reduced fibrin deposition in the CLP mice lungs. There is a possibility that the inflammation in CLP mice lungs was reduced, leading to decreased fibrin deposition.

Activating the AKT/mTOR signaling pathway in sepsis can lead to inflammatory response and mediate organ dysfunction [13, 14]. Studies have pointed out that the relationship between the activation of AKT/mTOR and the expression of TF has been confirmed [15, 16]. Additionally, STAT3, a nuclear transcription factor, is regulated by the AKT/mTOR signaling pathway [17]. It is also possible to suppress the expression of TF by inhibiting transcription factor STAT3 [18]. Our study showed that PL inhibits the phosphorylation of AKT, mTOR, and STAT3 proteins and reduces the nuclear import of p-STAT3 in LPS-stimulated RAW264.7 cells. Therefore, we postulated that PL may improve sepsis' inflammatory response and coagulation indicators by inhibiting the AKT/mTOR signaling pathway.

CONCLUSIONS

In summary, PL could increase the survival rate of CLP mice. Moreover, PL could moderate coagulation indicators and alleviate lung inflammation in CLP mice. These positive effects may be mediated by inhibiting the activation of AKT/mTOR pathways. Whether PL protects other organs from sepsis and whether PL has other positive effects in sepsis treatment remain to be explored.

ACKNOWLEDGEMENTS

AUTHOR CONTRIBUTION

ZF performed the experiments and wrote the paper; XZ, YH, HZ, FY, and YS collected and analyzed the data; YL, LP, and WC designed the figure legends; HJ and SQ contributed to the drafting of the manuscript; DL, JB, and ZZ gave guidance on experimental technology; and JP conceived the study. All authors read and approved the final manuscript.

FUNDING

DATA AVAILABILITY

The datasets used and/or analyzed during the present study are available from the corresponding author on reasonable request.

DECLARATIONS

Ethics Approval The study was conducted by the Declaration of Helsinki and approved by Wenzhou Medical University Institutional Animal Care and Use Committees. The animal study protocol was approved by the Institutional Review Board (or Ethics Committee) of NAME OF INSTITUTE (YS2018-088, 2018.02.26).

Conflict of Interest The authors declare no competing interests.

REFERENCES

1. Reinhart, K., R. Daniels, N. Kissoon, F.R. Machado, R.D. Schachter, and S. Finfer. 2017. Recognizing sepsis as a global health priority - a WHO resolution. *New England Journal of Medicine* 377: 414–417. https://doi.org/10.1056/NEJMp1707170.

2. Shimamura, K., K. Oka, M. Nakazawa, and M. Kojima. 1983. Distribution patterns of microthrombi in disseminated intravascular coagulation. *Archives of Pathology and Laboratory Medicine* 107: 543–547.

3. Ackermann, M., S.E. Verleden, M. Kuehnel, A. Haverich, T. Welte, F. Laenger, A. Vanstapel, C. Werlein, H. Stark, A. Tzankov, *et al*. 2020. Pulmonary vascular endothelialitis, thrombosis, and angiogenesis in COVID-19. *New England Journal of Medicine* 383: 120–128. https://doi.org/10.1056/NEJMoa2015432.

4. Chen, W., and J.Y. Pan. 2021. Anatomical and pathological observation and analysis of SARS and COVID-19: Microthrombosis is the main cause of death. *Biol Proced Online* 23: 4. https://doi.org/10.1186/s12575-021-00142-y.

5. Iba, T., M. Levi, and J.H. Levy. 2020. Sepsis-induced coagulopathy and disseminated intravascular coagulation. *Seminars in Thrombosis and Hemostasis* 46: 89–95. https://doi.org/10.1055/s-0039-1694995.

6. Gando, S., M. Levi, and C.H. Toh. 2016. Disseminated intravascular coagulation. *Nature Reviews. Disease Primers* 2: 16037. https://doi.org/10.1038/nrdp.2016.37.

7. Rosseau, S., P. Hammerl, U. Maus, H.D. Walmrath, H. Schütte, F. Grimminger, W. Seeger, and J. Lohmeyer. 2000. Phenotypic characterization of alveolar monocyte recruitment in acute respiratory distress syndrome. *American Journal of Physiology. Lung Cellular and Molecular Physiology* 279: L25-35. https://doi.org/10.1152/ajplung.2000.279.1.L25.

8. Zhang, H., L. Zeng, M. Xie, J. Liu, B. Zhou, R. Wu, L. Cao, G. Kroemer, H. Wang, T.R. Billiar, *et al*. 2020. TMEM173 drives lethal coagulation in sepsis. *Cell Host & Microbe* 27: 556-570. e556. https://doi.org/10.1016/j.chom.2020.02.004.

9. Levi, M., and T. van der Poll. 2010. Inflammation and coagulation. *Critical Care Medicine* 38: S26-34. https://doi.org/10.1097/CCM.0b013e3181c98d21.

10. van der Poll, T., M. Levi, C.E. Hack, H. ten Cate, S.J. van Deventer, A.J. Eerenberg, E.R. de Groot, J. Jansen, H. Gallati, H.R. Büller, *et al*. 1994. Elimination of interleukin 6 attenuates coagulation activation in experimental endotoxemia in chimpanzees. *Journal of Experimental Medicine* 179: 1253–1259. https://doi.org/10.1084/jem.179.4.1253.

11. Grimaldi, D., E.W. Goicoechea Turcott, and F.S. Taccone. 2016. IL-1 receptor antagonist in sepsis: New findings with old data? *Journal of Thoracic Disease* 8: 2379–2382. https://doi.org/10.21037/jtd.2016.08.51.

12. Coughlin, S.R. 2000. Thrombin signalling and protease-activated receptors. *Nature* 407: 258–264. https://doi.org/10.1038/35025229.

13. Schmitz, F., A. Heit, S. Dreher, K. Eisenächer, J. Mages, T. Haas, A. Krug, K.P. Janssen, C.J. Kirschning, and H. Wagner. 2008.

Mammalian target of rapamycin (mTOR) orchestrates the defense program of innate immune cells. *European Journal of Immunology* 38: 2981–2992. https://doi.org/10.1002/eji.200838761.

14. Chen, H., J. Zhu, Y. Liu, Z. Dong, H. Liu, Y. Liu, X. Zhou, F. Liu, and G. Chen. 2015. Lipopolysaccharide induces chronic kidney injury and fibrosis through activation of mTOR signaling in macrophages. *American Journal of Nephrology* 42: 305–317. https://doi.org/10.1159/000441506.

15. Hu, C., L. Huang, C. Gest, X. Xi, A. Janin, C. Soria, H. Li, and H. Lu. 2012. Opposite regulation by PI3K/Akt and MAPK/ERK pathways of tissue factor expression, cell-associated procoagulant activity and invasiveness in MDA-MB-231 cells. *Journal of Hematology & Oncology* 5: 16. https://doi.org/10.1186/1756-8722-5-16.

16. Eisenreich, A., R. Malz, W. Pepke, Y. Ayral, W. Poller, H.P. Schultheiss, and U. Rauch. 2009. Role of the phosphatidylinositol 3-kinase/protein kinase B pathway in regulating alternative splicing of tissue factor mRNA in human endothelial cells. *Circulation Journal* 73: 1746–1752. https://doi.org/10.1253/circj.cj-99-0225.

17. Liu, Y., S. Deng, Z. Zhang, Y. Gu, S. Xia, X. Bao, X. Cao, and Y. Xu. 2020. 6-Gingerol attenuates microglia-mediated neuroinflammation and ischemic brain injuries through Akt-mTOR-STAT3 signaling pathway. *European Journal of Pharmacology* 883: 173294. https://doi.org/10.1016/j.ejphar.2020.173294.

18. Xu, S., X. Pan, L. Mao, H. Pan, W. Xu, Y. Hu, X. Yu, Z. Chen, S. Qian, Y. Ye, *et al*. 2020. Phospho-Tyr705 of STAT3 is a therapeutic target for sepsis through regulating inflammation and coagulation. *Cell Communication and Signaling* 18. https://doi.org/10.1186/s12964-020-00603-z.

19. Grover, S.P., and N. Mackman. 2018. Tissue factor: An essential mediator of hemostasis and trigger of thrombosis. *Arteriosclerosis, Thrombosis, and Vascular Biology* 38: 709–725. https://doi.org/10.1161/atvbaha.117.309846.

20. Zeerleder, S., C.E. Hack, and W.A. Wuillemin. 2005. Disseminated intravascular coagulation in sepsis. *Chest* 128: 2864–2875. https://doi.org/10.1378/chest.128.4.2864.

21. Bezerra, D.P., F.O. Castro, A.P. Alves, C. Pessoa, M.O. Moraes, E.R. Silveira, M.A. Lima, F.J. Elmiro, and L.V. Costa-Lotufo. 2006. *In vivo* growth-inhibition of sarcoma 180 by piplartine and piperine, two alkaloid amides from Piper. *Brazilian Journal of Medical and Biological Research* 39: 801–807. https://doi.org/10.1590/s0100-879x2006000600014.

22. Rodrigues, R.V., D. Lanznaster, D.T. Longhi Balbinot, M. Gadotti Vde, V.A. Facundo, and A.R. Santos. 2009. Antinociceptive effect of crude extract, fractions and three alkaloids obtained from fruits of Piper tuberculatum. *Biological &/and Pharmaceutical Bulletin* 32: 1809–1812. https://doi.org/10.1248/bpb.32.1809.

23. Ku, S.K., J.A. Kim, and J.S. Bae. 2014. Vascular barrier protective effects of piperlonguminine *in vitro* and *in vivo*. *Inflammation Research* 63: 369–379. https://doi.org/10.1007/s00011-014-0708-6.

24. Park, B.S., D.J. Son, W.S. Choi, G.R. Takeoka, S.O. Han, T.W. Kim, and S.E. Lee. 2008. Antiplatelet activities of newly synthesized derivatives of piperlongumine. *Phytotherapy Research* 22: 1195–1199. https://doi.org/10.1002/ptr.2432.

25. Xu, P., J. Xiao, and S. Chi. 2021. Piperlongumine attenuates oxidative stress, inflammatory, and apoptosis through modulating the GLUT-2/4 and AKT signaling pathway in streptozotocin-induced diabetic rats. *Journal of Biochemical and Molecular Toxicology* 35: 1–12. https://doi.org/10.1002/jbt.22763.

26. Huang, Y., F. Wang, H. Li, S. Xu, W. Xu, X. Pan, Y. Hu, L. Mao, S. Qian, and J. Pan. 2019. Inhibition of fibroblast growth factor receptor by AZD4547 protects against inflammation in

septic mice. *Inflammation* 42: 1957–1967. https://doi.org/10.1007/s10753-019-01056-4.

27. Toscano, M.G., D. Ganea, and A.M. Gamero. 2011. Cecal ligation puncture procedure. *Journal of Visualized Experiments*. https://doi.org/10.3791/2860.

28. Sun, S.C. 2017. The non-canonical NF-κB pathway in immunity and inflammation. *Nature Reviews Immunology* 17: 545–558. https://doi.org/10.1038/nri.2017.52.

29. Levi, M., and T. van der Poll. 2017. Coagulation and sepsis. *Thrombosis Research* 149: 38–44. https://doi.org/10.1016/j.thromres.2016.11.007.

30. Kumar, V. 2018. Targeting macrophage immunometabolism: Dawn in the darkness of sepsis. *International Immunopharmacology* 58: 173–185. https://doi.org/10.1016/j.intimp.2018.03.005.

31. Fan, E.K.Y., and J. Fan. 2018. Regulation of alveolar macrophage death in acute lung inflammation. *Respiratory Research* 19: 50. https://doi.org/10.1186/s12931-018-0756-5.

32. Liu, Y.C., X.B. Zou, Y.F. Chai, and Y.M. Yao. 2014. Macrophage polarization in inflammatory diseases. *International Journal of Biological Sciences* 10: 520–529. https://doi.org/10.7150/ijbs.8879.

33. Wu, C., W. Lu, Y. Zhang, G. Zhang, X. Shi, Y. Hisada, S.P. Grover, X. Zhang, L. Li, B. Xiang, *et al*. 2019. Inflammasome activation triggers blood clotting and host death through pyroptosis. *Immunity* 50: 1401-1411.e1404. https://doi.org/10.1016/j.immuni.2019.04.003.

34. Franco, R.F., E. de Jonge, P.E. Dekkers, J.J. Timmerman, C.A. Spek, S.J. van Deventer, P. van Deursen, L. van Kerkhoff, B. van Gemen, H. ten Cate, *et al*. 2000. The *in vivo* kinetics of tissue factor messenger RNA expression during human endotoxemia: Relationship with activation of coagulation. *Blood* 96: 554–559.

35. Nadeem, A., S.F. Ahmad, N.O. Al-Harbi, K.E. Ibrahim, F. Alqahtani, W.A. Alanazi, H.M. Mahmood, S. Alsanea, and S.M. Attia. 2021. Bruton's tyrosine kinase inhibition attenuates oxidative stress in systemic immune cells and renal compartment during sepsis-induced acute kidney injury in mice. *International Immunopharmacology* 90: 107123. https://doi.org/10.1016/j.intimp.2020.107123.

36. Al-Harbi, N.O., A. Nadeem, S.F. Ahmad, M.R. Alotaibi, A.F. AlAsmari, W.A. Alanazi, M.M. Al-Harbi, A.M. El-Sherbeeny, and K.E. Ibrahim. 2018. Short chain fatty acid, acetate ameliorates sepsis-induced acute kidney injury by inhibition of NADPH oxidase signaling in T cells. *International Immunopharmacology* 58: 24–31. https://doi.org/10.1016/j.intimp.2018.02.023.

37. Al-Harbi, N.O., A. Nadeem, S.F. Ahmad, M.M. Alanazi, A.A. Aldossari, and F. Alasmari. 2019. Amelioration of sepsis-induced acute kidney injury through inhibition of inflammatory cytokines and oxidative stress in dendritic cells and neutrophils respectively in mice: Role of spleen tyrosine kinase signaling. *Biochimie* 158: 102–110. https://doi.org/10.1016/j.biochi.2018.12.014.

38. Nadeem, A., S.F. Ahmad, N.O. Al-Harbi, M.M. Al-Harbi, K.E. Ibrahim, S. Kundu, S.M. Attia, W.A. Alanazi, and S.D. AlSharari. 2019. Inhibition of spleen tyrosine kinase signaling protects against acute lung injury through blockade of NADPH oxidase and IL-17A in neutrophils and γδ T cells respectively in mice. *International Immunopharmacology* 68: 39–47. https://doi.org/10.1016/j.intimp.2018.12.062.

39. Nadeem, A., N.O. Al-Harbi, S.F. Ahmad, M.M. Al-Harbi, A.S. Alhamed, A.S. Alfardan, M.A. Assiri, K.E. Ibrahim, and H. Albassam. 2020. Blockade of interleukin-2-inducible T-cell kinase signaling attenuates acute lung injury in mice through adjustment of pulmonary Th17/Treg immune responses and reduction of oxidative stress. *International Immunopharmacology* 83: 106369. https://doi.org/10.1016/j.intimp.2020.106369.

40. Rothmeier, A.S., P. Marchese, B.G. Petrich, C. Furlan-Freguia, M.H. Ginsberg, Z.M. Ruggeri, and W. Ruf. 2015. Caspase-1-mediated pathway promotes generation of thromboinflammatory microparticles. *The Journal of Clinical Investigation* 125: 1471–1484. https://doi.org/10.1172/jci79329.

41. Yang, X., X. Cheng, Y. Tang, X. Qiu, Y. Wang, H. Kang, J. Wu, Z. Wang, Y. Liu, F. Chen, *et al.* 2019. Bacterial endotoxin activates the coagulation cascade through gasdermin D-dependent phosphatidylserine exposure. *Immunity* 51: 983-996.e986. https://doi.org/10.1016/j.immuni.2019.11.005.

42. Morrissey, J.H., B.G. Macik, P.F. Neuenschwander, and P.C. Comp. 1993. Quantitation of activated factor VII levels in plasma using a tissue factor mutant selectively deficient in promoting factor VII activation. *Blood* 81: 734–744.

43. Phua, J., J.R. Badia, N.K. Adhikari, J.O. Friedrich, R.A. Fowler, J.M. Singh, D.C. Scales, D.R. Stather, A. Li, A. Jones, *et al.* 2009. Has mortality from acute respiratory distress syndrome decreased over time?: A systematic review. *American Journal of Respiratory and Critical Care Medicine* 179: 220–227. https://doi.org/10.1164/rccm.200805-722OC.

44. Bao, S., M.J. Liu, B. Lee, B. Besecker, J.P. Lai, D.C. Guttridge, and D.L. Knoell. 2010. Zinc modulates the innate immune response *in vivo* to polymicrobial sepsis through regulation of NF-kappaB. *American Journal of Physiology. Lung Cellular and Molecular Physiology* 298: L744-754. https://doi.org/10.1152/ajplung.00368.2009.

45. Nadeem, A., N.O. Al-Harbi, A.S. Alfardan, S.F. Ahmad, A.F. AlAsmari, and M.M. Al-Harbi. 2018. IL-17A-induced neutrophilic airway inflammation is mediated by oxidant-antioxidant imbalance and inflammatory cytokines in mice. *Biomedicine & Pharmacotherapy* 107: 1196–1204. https://doi.org/10.1016/j.biopha.2018.08.123.